Nitrogen transformations along a shallow subterranean estuary

Mathilde Couturier[1,2], Gwendoline Tommi-Morin[1,2], Maude Sirois[1,3], Alexandra Rao[3], Christian Nozais[2], Gwénaëlle Chaillou [1,2]

[1] Canada Research Chair on the Geochemistry of Coastal Hydrogeosystems, BOREAS, group on Nordic System, Département de Biologie, Chimie, Géographie, Université du Québec à Rimouski, Rimouski, G5L3A1, Canada
[2] Département de Biologie, Chimie, Géographie, Université du Québec à Rimouski, Rimouski, G5L3A1, Canada
[3] Institut des sciences de la mer de Rimouski, Université du Québec à Rimouski, Rimouski, Québec, G5L 3A1, Canada

Correspondence to: Mathilde Couturier (Mathilde.Couturier@uqar.ca)

Abstract. The transformations of chemical constituents in subterranean estuaries (STE) control the delivery of nutrient loads from coastal aquifer to the ocean. It is important to determine the processes and sources that alter nutrient concentrations at a local scale in order to estimate accurate regional and global nutrient fluxes *via* submarine groundwater discharge (SGD), particularly in boreal environments, where data are still very scarce. Here, the biogeochemical transformations of nitrogen (N) species were examined within the STE of a microtidal boreal sandy beach located in the Magdalen Islands (Québec, Canada). This study revealed the vertical and horizontal distribution of nitrate (NO_3^-), nitrite (NO_2^-), ammonia (NH_4^+), dissolved organic nitrogen (DON) and total dissolved nitrogen (TDN) measured in beach groundwater during four spring seasons (June 2011, 2012, 2013 and 2015) when aquifer recharge was maximal after snowmelt. Inland groundwater supplied high concentrations of NO_x and DON to the STE, whereas inputs from seawater infiltration were very limited. Non-conservative behaviour was observed along the groundwater flow path, leading to low NO_x and high NH_4^+ concentrations in the discharge zone. The long transit time of groundwater within the beach (~166 days), coupled with oxygen-depleted conditions and high carbon concentrations created a favourable environment for N transformations such as heterotrophic and autotrophic denitrification and ammonium production. Biogeochemical pathways led to a shift in nitrogen species along the flow path from NO_x-rich to NO_x-poor groundwater. An estimate of SGD fluxes of N was determined to account for biogeochemical transformations within the STE based on a N-species inventory and Darcy's flow. Fresh inland groundwater delivered 37 mol NO_x y^{-1} and per m of shoreline and 63 mol DON m^{-1} y^{-1} to the STE, and NH_4^+ input was negligible. Near the discharge zone, the potential export of N species was estimated around 140, 1.5 and 33 mol y^{-1} per meter of shoreline for NH_4^+, NO_x and DON respectively. In contrast to the fresh inland groundwater,

the N load of beach groundwater near the discharge zone was dominated by NH_4^+ and DON. Our study shows the importance of tidal sands in the biogeochemical transformation of terrestrial N pool. This local export of bioavailable N probably supports benthic production and higher trophic levels leading to its rapid transformation in surface sediments and coastal waters.

5   1 Introduction

Land–ocean interfaces are critical transition zones that may affect the ecology and quality of coastal ecosystems (Schlacher and Connolly, 2009). Chemical constituents in submarine groundwater discharge (SGD) are now widely recognized to have a significant impact on coastal ecosystems (Knee and Jordan, 2013; McCoy and Corbett, 2009; Null et al., 2012; Slomp and Van Cappellen, 2004). SGD is conventionally defined as "any flow of water out across the seafloor without regards to its composition and its origin" (Burnett et al., 2006). Thus, before entering coastal waters, fresh groundwater travels through the shallow subterranean estuary (STE) (Moore, 1999), a region where mixing between fresh and marine groundwater promotes biogeochemical processes that can lead to rapid changes in nutrient concentrations and induce non-conservative input or removal (Gonneea and Charette, 2014). The STE supports extensive chemical reactions near the discharge interface and is often assumed to be a non-steady-state system (Kroeger and Charette, 2008). Continental factors (e.g., local hydrogeology, recharge, precipitation) as well as marine factors (e.g., tidal and wave pumping, hydrography, and density) induce temporal and spatial variability in biogeochemical conditions (see Santos et al. 2012 and references therein). The mixing zone is subject to oscillating conditions, with rapid changes in oxygen saturation, redox potential, and organic matter input controlled by tidal stage and amplitude, sea level as well as seasonal water-table fluctuations (Abarca et al., 2013; Gonneea et al., 2013, Heiss et al., 2014; Robinson et al., 2014). These physical processes are likely to impact the distribution and biogeochemical reactivity of many dissolved constituents (Beck et al., 2007; Kroeger and Charette, 2008). In this context, the STE can either be a source of nutrients or act as a barrier and limit nutrient discharge to coastal environments. Assessing the role of the STE in nutrient transformations is crucial to better quantifying global chemical fluxes *via* SGD (Moore, 2010).

Rivers have long been considered the main conveyors of N to the ocean (Seitzinger et al., 2005, and references therein). Beusen et al. (2013) recently provided evidence that SGD also plays a major role in regional and global marine N cycles. N loads from SGD to near-shore ecosystems were estimated to be 4 Tg N y^{-1} (Voss et al., 2013), and the role of SGD in coastal eutrophication has also been demonstrated (Valiela et al., 1990). These N loads may be an important factor in the

5   development of harmful algal blooms in coastal waters (Anderson et al., 2008; Glibert et al., 2014). Fresh groundwater is often rich in nutrients and other materials from anthropogenic inputs due to coastal development (agriculture, urbanization) (Howarth and Marino, 2006; Null et al., 2012; Rocha et al., 2015), and models predict a 20% increase in N loads from SGD within the next few decades due to coastal development (Beusen et al., 2013).

Estimates of nutrient loads from the SGD to the coastal ocean have often been based on nutrient concentrations in fresh

10   groundwater, with the assumption that nutrient transport through the STE is conservative (Burnett et al., 2006). However, numerous studies have demonstrated that concentrations of dissolved N change throughout the STE because of biological and chemical reactions (Beck et al., 2007; Loveless and Oldham, 2010; Moore, 2010; Santos et al., 2009). Variations in oxygen and organic matter input along the hydraulic gradient lead to a combination of heterotrophic processes that can enhance or attenuate the export of N to the coastal ocean (Santoro, 2010). For example, in the Gulf of Mexico (Turkey Point,

15   Florida), the STE acts as a source of ammonium because remineralization of marine organic matter throughout the STE provides nutrients to the SGD exported to the embayment (Santos et al., 2008). In Waquoit Bay (Cape Cod, Massachusetts), Kroeger and Charette (2008) demonstrated that ammonium accumulates in the STE because remineralization of organic matter transported by marine and fresh groundwater outpaces nitrification. In contrast, based on the N attenuation observed in a shallow STE due to denitrification (Cockburn Sound, Australia), Loveless and Oldham (2010) calculated nitrate loads to

20   coastal waters that were 1–2 times lower than previous estimates based on nutrient concentrations from fresh groundwater. As these studies show, ignoring non-conservative mixing can lead to an over- or under-estimation of nutrient loads to coastal waters (Beck et al., 2007).

STEs are transient systems where steady state, and thus the classical diagenetic sequence of redox reactions, are rarely achieved (Sundby, 2006). In transient systems, diagenetic reactions reflect redox oscillations and environmental conditions

25   far from steady state. Redox oscillations, with alternating oxic and anoxic conditions in sediments, allow coupled

nitrification–denitrification to take place in the same location within the sediment (Aller, 1994). Alternative pathways of nitrate reduction, such as dissimilatory nitrate reduction to ammonium (DNRA) and ANAMMOX, have also been reported in the STE (Erler et al., 2014; Kroeger and Charette, 2008; Rocha et al., 2009; Sáenz et al., 2012). Many of these processes transform dissolved inorganic nitrogen (DIN) and dissolved organic nitrogen (DON) along the groundwater flow path. DON

5   is assumed to be from natural rather than anthropogenic sources and is often neglected (Hansell and Carlson, 2014). Nevertheless, DON concentrations can be high in SGD and should be considered (Kroeger et al., 2007; Santos et al., 2014). Martinique Beach, located in the Magdalen Islands (Québec, Canada) in the southern limit of the boreal climatic zone, is exposed to little or no external contamination. Site-specific studies in boreal and cold environments are still scarce and climate and hydrology change rapidly in cold climates (Hinzman et al., 2005). Thus nutrient fluxes by SGD to the coastal

10   ocean in boreal regions and their contribution at local and global scales remains to be elucidated. The objective of this four-year study was to investigate the spatial and temporal variation of N species (inorganic and organic N) through a shallow boreal STE, from inland groundwater to coastal ocean. SGD fluxes of the different N species that are discharged to coastal waters by shallow groundwater at this specific-site were also estimated.

2 Materials and methods

15   **2.1 Study area**

Martinique Beach is located on the main island of the Magdalen Islands archipelago in the Gulf of St. Lawrence (Québec, Canada; Fig.1). The Martinique Beach system originates from a recent transgression sequence. Rapid rates of sea-level rise along the Atlantic coast of Canada over the middle to late Holocene buried the unconfined Permian sandstone aquifer that is now covered by tidal sediment (Gehrels, 1994; Scott et al., 1995a, 1995b). The site experiences semi-diurnal tides with a

20   mean range of 0.8 m and a maximum range of 1.7 m during spring tide. The archipelago has no rivers, thus the aquifer recharge is only from rain and snow, with the highest recharge during spring snowmelt. The mean yearly recharge is about 230 mm (Madelin'Eau, 2004). Because groundwater constitutes the only source of drinking water in the archipelago, the hydrogeology is well known and the aquifer constantly monitored (Chaillou et al., 2012; Madelin'Eau, 2007, 2009, 2011). Since anthropogenic pressures like urbanization and agriculture are limited on the archipelago, the main sources of N

4

contamination are from residential and recreational areas. Therefore, Martinique Beach is an ideal system in which to study N transformations in a boreal microtidal subterranean estuary.

The Martinique Beach STE acts as a shallow unconfined aquifer at the nearshore limit of the Permian Aquifer; it releases both fresh and recirculated saline groundwater to the coastal embayment (Chaillou et al., 2016). It is a low-energy beach under a micro-tidal regime (Jackson et al., 2002; Masselink and Short, 1993). The upper centimeters (20 cm) of the beach consist of marine sands with a median particle size of 0.30 mm (silt content <5%), mainly composed of quartz (95%). The hydraulic conductivity of this sedimentary unit is about 11.40 ± 4.40 m d^{-1} (Chaillou et al., 2016). Lower hydraulic conductivity was measured in the underlying sandstone aquifer (K ~1.80 m d^{-1}; Madelin'Eau, 2007), which is composed of fine silicate and aluminosilicate sands with Fe-coated silicate grains (Chaillou et al., 2014). These two layers are organic-poor (total organic carbon [TOC] < 0.20% weight percent (w.t.) and total nitrogen [TN] < 0.10% w.t.; Chaillou et al., 2014). In the landward part of the beach, however, an old-age soil horizon dated to ~900 B.P. (^{14}C dating; Juneau, 2012) occurs a few centimeters below the beach surface. This horizon is carbon-rich (TOC > 20% w.t.) but has a low nitrogen content (TN < 0.50% w.t.; Chaillou et al., 2014).

In the Magdalen Islands, the snowmelt leads to a high water table from April to June in the Permian sandstone aquifer (Madelin'Eau, 2004) and in the adjacent beach aquifer (Chaillou et al., 2016). Under these hydrologic conditions, the saline circulation cell and its associated mixing zone are spatially limited, and the inland hydraulic gradient is the main control of total SGD (Heiss and Michael, 2014; Robinson et al., 2007a). Based on the stable isotopes of water along the STE, Chaillou et al., (submitted) confirmed the contribution of only two water end-members (i.e., fresh meteoric groundwater and seawater) and the absence of additional septic tank seepages. They also highlighted the high contribution of fresh groundwater and the limited infiltration of seawater in shallow beach groundwater. The regional seaward fresh groundwater flow (Q_{inland}) of about 0.021 m^3 s^{-1} was estimated based on mean and multi-annual regional water table levels in spring 2013 from municipal wells (Chaillou et al., 2016). Q_{inland} is then the theoretical inland groundwater export from the Permian sandstone aquifer to the Martinique beach. In Martinique beach, fresh groundwater flow was also evaluated based on a mean hydraulic gradient through the 50m-length of the beach. This specific flow (Q_{beach}) was 0.029 m^3 s^{-1}, suggesting that fresh inland groundwater flux contributes to at least 70% of the water flow discharging to the coastal waters.

2.2 Groundwater sampling

Sampling was carried out in June 2011, 2012, 2013, and 2015 along a 50 m cross-shore transect. In 2011 and 2012, groundwater samples were collected in the landward part of the STE. In 2013 and 2015, we focused on the intertidal and discharge zone, where fresh meteoric groundwater comes in contact with recirculated seawater. Groundwater extraction was

5 done using multi-level samplers in 2.5 m long PVC pipes (Fig. 1), similar to those described by Martin et al. (2003). Groundwater was collected at 10, 30, 50, 80, 100, 150, 190, and 230 cm below the beach surface. Samplers were re-inserted at the same locations each year using DGPS coordinates. To allow sediments around the samplers to reach equilibrium, sampling started two days after their insertion. Groundwater was sampled using a peristaltic pump, and physicochemical parameters (pH, temperature, oxygen, salinity) were measured directly using an on-line flow cell with a calibrated multi-

10 parameter probe (600QS, YSI Inc.). Oxygen measurements are not available for 2015, due to sensor malfunction. After stabilization of physico-chemical parameters, all groundwater samples were filtered through a 0.2 µm polypropylene capsule filter. Samples for nutrient analyses (NH_4^+, NO_3^-, and NO_2^-) were stored in acid-washed polyethylene tubes that were rapidly frozen for later analysis; samples for total dissolved iron were stored at 4°C in 50 mL acid-washed polyethylene tubes and acidified with 50 µL of 10% HNO_3; and total dissolved nitrogen (TDN) samples were stored in baked 7 mL vials and

15 acidified with 25 µL of high purity 10% HCl. TDN measurements were only performed in 2012. Groundwater end-member samples were collected in the manner described above from four private and municipal wells (2 or 3 replicates per well) located 50 to 2000 m landward of the most inland sampler in the sandstone aquifer. Seawater end-member samples (N=6) were collected about 50 cm above the seabed using a submersible pump at about 900 m offshore in Martinique Bay.

2.3 Chemical analyses

20 NH_4^+ samples were measured by flow injection gas exchange–conductivity analysis based on the method described by Hall and Aller (1992). The precision was ± 5% with a detection limit of 0.1 µmol L^{-1}. NO_3^- and NO_2^-, referred to as NO_x, were analysed by the colorimetric method developed by Schnetger and Lehners (2014) and measured with a powerwave XS2 microplate spectrophotometer. The precision was 2% and the limit of detection was 0.4 µmol L^{-1}. DIN was calculated as the sum of NH_4^+, NO_3^-, and NO_2^-. TDN was analysed in 2012 by high temperature combustion (HTC) using a Total Organic

25 Carbon analyser (TOC-vpn, Shimadzu) with a TNM-1 module, and a precision of 2%. Dissolved Organic Nitrogen (DON)

6

was calculated as the difference between TDN and DIN (i.e., DON = TDN − [NH_4^+ + NO_x]). DON calculations were only possible in 2012 based on TDN measurements. The DON measurement is still problematic since it combines the analytical errors and uncertainties of the three analyses. Nevertheless, there is currently no single accepted method for the measurement of DON (Hansell and Carlson, 2014). Here we estimated the precision to be around 10%. Dissolved iron was analysed using a 5100PC Flame Atomic Absorption spectrophotometer (5100ZL Zeeman Furnace). Analytical uncertainties were <5%.

3 Results

3.1 Distribution of salinity and oxygen saturation

Previous studies have already discussed the distribution of physico-chemical parameters along the groundwater flow path at Martinique Beach based on 2012 and 2013 data (Chaillou et al., 2014, 2016; Couturier et al., 2016). Here, we will briefly present an overview of the salinity and redox conditions in the STE (Fig. 2).

In 2011 and 2012, the landward part of the STE was mostly characterized by suboxic freshwater (dissolved oxygen [DO] < 20%, salinity < 10). The discharge zone with the saline circulation cell was salty and oxygenated ([DO] > 60%, salinity > 20). A sharp salinity gradient occurred below the saline circulation cell, with salinity falling to 0 within the upper 50 cm of the sediment. In 2013 and 2015, the focus on the intertidal zone confirmed the occurrence of a small saline circulation cell with sharp gradients of salinity and DO along its perimeter. Fresh and suboxic water were recurrent at 60 cm below the surface in the discharge zone of the beach. A mixing zone composed of brackish water (salinity comprised between 7 and 15) occurred along the perimeter of the saline circulation cell resulting from a mixture of fresh and saline groundwater. This mixing zone appeared to be depleted in DO ([DO] < 20%). The rest of the system was composed of fresh groundwater. In 2013, some measurements showing high DO concentrations in the deepest samples may indicate atmospheric contamination during sampling.

3.2 Nutrient distribution from inland groundwater to beach groundwater

The concentrations of NO_x ($\Sigma NO_3^- + NO_2^-$) measured in four inland wells ranged from 14 to 94 µmol L^{-1} with a mean concentration of 65.5 ± 26.7 µmol L^{-1} (Table 1). In the near shore well, located 50 m from the shoreline, the concentration reached 20 µmol L^{-1}. NH_4^+ concentrations were low, with concentrations varying between 0 and 1 µmol L^{-1}. The fresh inland

groundwater end-member was rich in TDN as measured in wells in 2012, with DON making up 53% of the TDN (i.e., DON = $110.9 \pm 3.4 \mu$mol L^{-1}). Compared to fresh inland groundwater, the seawater samples were largely depleted in NO$_x$ with a mean concentration of 0.5 ± 0.5 μmol L^{-1} (N=6, Table 1). NH$_4^+$ concentrations were also low with 0.8 ± 0.5 μmol L^{-1}. As in fresh inland groundwater, TDN in seawater was largely dominated by DON that represented ~80% of the N budget with a mean concentration of 7.3 ± 0.8 μmol L^{-1}. Overall, TDN concentrations in the seawater end-member were 20 times lower than in the groundwater end-member.

Within the STE, NO$_x$ concentrations were low (0–26 μmol L^{-1} with a mean concentration of 1.9 μmol L^{-1}). These concentrations were five times lower than those measured within the fresh groundwater end-member (Table 1, Fig. 3A). However, some samples collected in the deep and fresh part of the STE reached concentrations greater than 20 μmol L^{-1} (Fig. 3A). Such hot spots of NO$_x$ concentrations were also recorded in 2011 (up to 15.2 μmol L^{-1}), 2012 (up to 26.1 μmol L^{-1}), and 2015 (up to 19.5 μmol L^{-1}). In contrast to NO$_x$, NH$_4^+$ concentrations were high in the STE, with concentrations ranging from ~20 μmol L^{-1} to > 500 μmol L^{-1} (Fig. 3B), and up to 1056 μmol L^{-1} (2013, Fig. 3B). Ammonium (NH$_4^+$) concentrations measured in the STE were 1 to 1000 times higher than end-member values (Table 1, Fig. 3B). In 2013, an area of high concentrations was observed in the mixing zone, in front of the saline circulation cell, where NH$_4^+$ concentrations reached values greater than 400 μmol L^{-1} (Fig. 3B). NH$_4^+$ concentrations were still high in the saline circulation cell (e.g., 84–92 μmol L^{-1}), and these were also high compared to the overlying seawater end-member (Table 1). NH$_4^+$ concentrations decreased sharply with depth in the mixing zone. For example, in June 2013 maximum NH$_4^+$ concentrations were around 400 μmol L^{-1} at 30 cm below the beach surface of the intertidal zone and decreased to 50 μmol L^{-1} at 230 cm (Fig. 3B). NH$_4^+$ was the main TDN species in the STE (on average NH$_4^+$ concentrations accounted for 60% of TDN in all samples). Thus, in 2012, the TDN distribution was quite similar to the NH$_4^+$ distribution (Fig. 4), with high values in the mixing zone. TDN decreased sharply below the saline circulation cell and the mixing zone; values ranged from 50 to 100 μmol L^{-1} and dropped below detection below the saline circulation cell. DON represented 31% of the TDN in beach groundwater, and the highest concentrations were observed in the mixing zone (>200 μmol L^{-1}, Fig. 4). DON levels decreased below the saline circulation cell, with concentrations close to 0.

N species showed different distributions relative to groundwater salinity and DO saturation along the STE (Fig. 5). N species were characterized by non-conservative behaviour relative to the theoretical two-end-member mixing between seawater and fresh inland groundwater. NO_x declined from 60 µmol L^{-1} in fresh inland groundwater to concentrations below detection in brackish and saline groundwater (Fig. 5A). The highest concentrations of NO_x were encountered when DO saturation was below 60%. While dissolved NO_x showed removal in the flow path, NH_4^+ exhibited excess concentrations relative to conservative mixing between the two end-members (Fig. 5B). NH_4^+ concentrations clearly showed strong production along the salinity gradient of the STE. The highest concentrations of NH_4^+ occurred mainly under suboxic conditions (DO < 20%) and decreased significantly with increased DO (p value < 0.05). Both NH_4^+ and NO_x were observed in 81 of 245 samples (~33% of the data set). These samples were mainly located just below the saline circulation cell and the associated mixing zone, where oxygen-depleted conditions prevailed ([DO] < 20%). In contrast to the behaviour of NO_x and NH_4^+, TDN and DON exhibited a distinct trend along the salinity gradient: (i) they fell below the theoretical mixing line in fresh and brackish waters (salinity 0 - 10) and this removal occurred in suboxic–anoxic conditions, and (ii) their concentrations increased above the theoretical mixing line in saline waters (salinity > 10). There was no significant relationship with DO.

Total dissolved iron concentrations were high in the STE and ranged from 1 to 2700 µmol L^{-1} with a mean concentration of 520 µmol L^{-1} (Fig. 6). Concentrations increased sharply with depth and below the saline circulation cell. Concentrations of dissolved iron in the upper meter of the STE and in the saline circulation cell were lower, but still high (from 1 to 100 µmol L^{-1}) compared to the overlaying water.

4 Discussion

4.1 Biogeochemical controls of DIN concentrations along the groundwater flow path

The non-conservative behaviour of DIN along the groundwater flow path influences the nutrient concentration in discharging groundwater, while at the same time making it difficult to estimate the flux of groundwater-derived DIN to the coastal ocean (Johannes, 1980; Moore, 2010; Valiela et al., 1990). The calculation of chemical fluxes using samples from inland wells may result in significant errors in estimated chemical fluxes. Processes occurring in the STE must be elucidated to improve our understanding of the role of the STE in altering groundwater-derived N. The DIN pool changed from NO_x-

rich groundwater in the aquifer to NH_4^+-rich groundwater in the STE. In our study, NO_x represented 99% of the DIN pool in the fresh inland groundwater end-member but only 37% in the seawater end-member. In the next section, the potential biogeochemical mechanisms controlling the N pool along the flow path are explored.
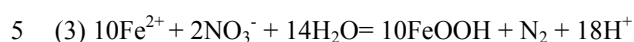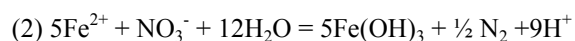
4.1.1 Nitrate loss along the STE

5   NO_x concentrations were low within the STE in contrast to the high concentrations measured in fresh inland groundwater. There was a strong attenuation in NO_x, with mean concentrations of 60 µmol L^{-1} in inland wells (~500 to 1500 m from the shoreline) dropping to ~20 µmol L^{-1} in the nearshore well (50 m from the shoreline) and to 2 µmol L^{-1} in the STE, near the discharge zone. Such attenuation of NO_x is common in groundwater (Rivett et al., 2008) and denitrification is generally recognized as the most significant mass removal process along the flow path (Korom, 1992). Denitrification is central to the

10   nitrogen cycle in the subsurface groundwater environment. It involves the reduction of NO_x to N_2 gas *via* a chain of microbial reduction reactions.

As oxygen-depleted conditions and high DOC concentrations are encountered along the STE (Couturier et al., 2016), denitrification may be one of the processes driving rapid groundwater-born NO_x loss. The stoichiometry of nitrate reduction and the oxidation of organic matter by denitrification, given by Jørgensen et al. (2014), is as follows:

15   (1) $5CH_2O + 4NO_3^- + 4H^+ = 2N_2 + 5CO_2 + 7H_2O$
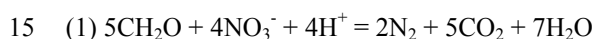
According to this stoichiometry, the mean concentration of DOC observed in the STE (i.e., 1940 µmol C L^{-1}; Couturier et al., 2016) could be used to reduce 1550 µmol L^{-1} of nitrate to dinitrogen by denitrification. With concentrations of NO_x around 20 µmol L^{-1} in the nearshore well, this means that all groundwater-borne NO_3^- may conceivably be reduced by DOC. However, even if the concentration of DOC in groundwater is high, Couturier et al. (2016) showed that DOM had a strong

20   terrestrial signature along the STE in Martinique Beach. This OC was characterized by a high molecular weight and was enriched in lignin-derived compounds. In an alluvial aquifer, Baker and Vervier (2004) confirmed that the rate of denitrification was best predicted by the concentration of low molecular weight organic acids compared to high molecular weight compounds. In an unconfined sandy aquifer, Postma et al. (1991) reported that nitrate reduction was minimal when OC was present as lignin and lignite fragments (i.e., as high molecular weight compounds). Thus, the terrestrial DOC present

25   in the Martinique Beach STE may not promote high rates of heterotrophic denitrification at the study site.

Nitrate reduction can be supported however by electron donors others than organic matter such as Fe^{2+} (Aller, 1994; Postma, 1990). There is evidence that groundwater containing Fe^{2+} contains little or no nitrate (Korom, 1992). The presence of reduced iron is assumed to facilitate the occurrence of denitrification according to reactions 2 and 3:

(2) $5Fe^{2+} + NO_3^- + 12H_2O = 5Fe(OH)_3 + \frac{1}{2} N_2 + 9H^+$

(3) $10Fe^{2+} + 2NO_3^- + 14H_2O = 10FeOOH + N_2 + 18H^+$

High DOC concentrations (Couturier et al., 2016) support the reductive dissolution of Fe-oxyhydroxides and led to total dissolved iron concentrations as high as 1000-1600 $\mu mol\ L^{-1}$, with concentrations reaching 2700 $\mu mol\ L^{-1}$ in deep groundwater below the saline circulation cell (Fig. 6). Thus Fe^{2+} can act as an electron donor and may have induced a loss of nitrates along the flow path. This autotrophic denitrification is most efficient in aquifers with low nitrate input (Postma et al., 1991) and in margin sediments (Anschutz et al., 2002; Chaillou et al., 2007; Hulth et al., 1999; Hyacinthe et al., 2001). The stoichiometry of reactions 2 and 3 shows that one mole of Fe^{2+} can reduce 0.2 moles of NO_3^-. Based on the range of Fe^{2+} concentrations measured along the transect, this process is capable of completely reducing groundwater-borne NO_x.

With a maximum groundwater flow rate of 0.029 $m^3\ s^{-1}$ in beach groundwater (Chaillou et al., 2016), the groundwater transit time through the STE (~50 m) is about 166 days, which is long enough to support denitrification reactions and subsequent N transformations. Hot spots of NO_x concentrations (e.g., 7.5 $\mu mol\ L^{-1}$ at 50 cm depth with [DO] < 10% in 2013, 15.2 $\mu mol\ L^{-1}$ at 80 cm depth with [DO] < 30% in 2012, in 2015; Fig. 3A) were likely the result of local and sporadic production rather than traces of groundwater-borne NO_x. The downward infiltration of oxygenated seawater by tides could be large enough to oxidize NH_4^+ and produce NO_3^- along the saline circulation cell. These concentrations of NO_3^- remained low (< 6 $\mu mol\ L^{-1}$) in the STE probably because of the multiple electron donors that can be used to reduce NO_3^- to N_2 under anoxic conditions (i.e., DOC, Fe^{2+}, NH_4^+, H_2S, and FeS).

4.1.2 Ammonium production along the STE

Mineralization of organic matter is likely the most important source of NH_4^+ in the Martinique Beach STE. DON measurements in 2012 were high (0–1481 $\mu mol\ L^{-1}$), with a mean value of 80 $\mu mol\ L^{-1}$. DON is a complex mixture of primarily uncharacterized compounds, of which 10 to 70% are estimated to be bioavailable (Seitzinger et al., 2002). DON bioavailability is often reported to be dependent on the nature of compounds (Sipler and Bronk, 2014). In the beach

11

groundwater, DON represented 39% of the TDN, so its mineralization by heterotrophic micro-organisms could be responsible for part of the NH_4^+ production in the STE (Kroeger et al., 2006). Ammonium production is mainly located upstream the saline circulation cell (Fig. 3B), and is linked to the presence of high DON concentrations as observed in June 2012 (Fig. 4). Because ammonification is highly dependent on the bioavailability of DON, it is difficult to estimate what

5   fraction of NH_4^+ could be derived from DON mineralization. Based on the estimate that 10 to 70% of DON is bioavailable as proposed by Seitzinger et al. (2002), mineralization of DON could lead to the production of 8 to 56 µmol L^{-1} of NH_4^+, which represents between 2 and 10% of the NH_4^+ concentration observed in beach groundwater.

In coastal sediments, where sulphate is not limiting, sulphate reduction produces NH_4^+ according to the following reaction:

(4) $53SO_4^{2-} + (CH_2O)_{106}(NH_3)_{16}(H_3PO_4) = 39CO_2 + 67HCO_3^- + 16\ NH_4^+ + 53HS^- + 39H_2O + HPO_4^{2-}$
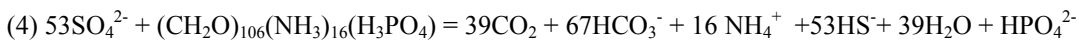
10   NH_4^+ was observed in samples with salinity > 4, with the highest concentrations (~1.25 mmol L^{-1}) at salinity around 15. At salinity 15, we estimate a SO_4^{2-} concentration of 12 mmol L^{-1} in beach surface groundwater, which is sufficient to produce 3.6 mmol L^{-1} NH_4^+ by sulphate reduction. This reaction could therefore explain the remainder of NH_4^+ production in beach groundwater.

The breakdown of macroalgal deposits derived from wave and tidal action in sediments can also increase N input to beach

15   groundwater (Kelaher and Levinton, 2003; Rossi et al., 2011) and can potentially add NH_4^+. At Martinique Beach, algal deposits were not specifically measured but were often observed after storm events. In addition, external contamination from wastewater or sceptic tank seepages cannot be completely excluded. Nevertheless, the absence of traces of NH_4^+ contamination in the landward part of the beach and the stable isotopes of water reported by Chaillou et al. (submitted) do not support an anthropogenic NH_4^+ input.

20   **4.2 Nutrient transport along the flow path**

The non-conservative behaviour of nutrients within the STE makes it difficult to estimate the export of nutrients to the coastal ocean. As pointed out in the review by Moore (2010), robust measurements of nutrient fluxes are needed on a site-specific scale to obtain accurate regional and global estimates. In non-conservative systems, however, the determination of appropriate nutrient end-member concentrations for flux calculations is not straightforward. Beck et al. (2007) previously

25   highlighted the need to closely scrutinize the biogeochemical processes in the STE to refine nutrient export fluxes to coastal

areas. Here, inorganic and organic N inventories were estimated along the groundwater flow path based on salinity. Then the potential nitrogen fluxes out of the STE were estimated and compared to the fresh inland groundwater-borne nutrient fluxes. Fluxes and inventories of the different N species along the groundwater flow path are summarized in Figure 7.

4.2.1 Nitrogen inventories

Nutrient inventories were calculated by integrating nutrient concentrations at sampling locations according to salinity and multiplying by the sediment porosity (i.e., 0.25; Chaillou et al. 2012). Salinity was used to delimit zones to calculate N-inventories along the flow path in deep fresh groundwater with low salinity (S< 5; N= 57), in the brackish beach groundwater (5<S<15; N=19) that runs parallel to the surficial saline circulation cell and, finally, in saline groundwater (S>15; N=15). Inorganic and organic nitrogen inventories are presented in Table 2.

In the inland groundwater wells, fresh groundwater was rich in DON (Table 1). DIN represented only 33% of the TDN, with NO_x making up 95% of the inorganic pool (Table 1). In the fresh beach groundwater (S<5), nutrient inventories showed that DON was still the main N species with an inventory of 18.7 µmol m^{-2} (Table 2) that represented more than 50% of the TDN pool. In DIN, a shift from NO_x to NH_4^+ occurred from the inland groundwater to deep fresh beach groundwater: NO_x became a negligible fraction (NO_x inventory < 0.5 µmol m^{-2}) whereas NH_4^+ was the main inorganic fraction representing 46, 53, and 61% of the TDN in fresh, brackish, and saline beach groundwater respectively.

NH_4^+ was clearly produced along the groundwater flow path through the STE. In brackish groundwater, a strong production of TDN was observed: DIN, NH_4^+, and DON increased by 169, 168, and 127%, respectively (Figure 7). Based on the previous work of Couturier et al. (2016), the source of nitrogen released in the STE is thought to be mineralization of terrestrial rather than marine organic matter. This strong *in situ* TDN production in the brackish beach groundwater altered the groundwater-borne N pool. Indeed, TDN concentrations in the saline circulation cell are much higher than the input from inland groundwater, even if this TDN is subsequently attenuate in surface sediment in the saline circulation cell due to biogeochemical processes and dilution (Table 2). Our findings showed that even if groundwater-borne TDN, in the form of NO_3^- and DON, was mostly attenuated along the groundwater flow path, a "new" N pool was produced within the STE as it was already observed for DOM (Couturier et al., 2016).

4.2.2 Nitrogen fluxes

The fresh groundwater-borne N fluxes to the STE have been calculated as the product of the mean DON, NO_x and NH_4^+ concentrations of the fresh inland groundwater end-member and the flow of fresh groundwater on shore (Chaillou et al. 2016). The fresh inland groundwater-derived N input estimated in this way was <0.07 mol m^{-1} y^{-1} and 37 mol m^{-1} y^{-1} for

5   NH_4^+ and NO_x respectively. Estimated DIN and DON fluxes are 37 mol m^{-1} y^{-1} and 63 mol m^{-1} y^{-1}, respectively (Table 3). The estimated groundwater-borne TDN flux was approximately 102 mol m^{-1} y^{-1}, corresponding to an annual N input of ~1700 kg along the 1200 m Martinique Beach shoreline. This flux is dominated by DON, and NO_x. Inland groundwater clearly acts as a source of nitrogen to the beach groundwater, as has been observed in other STEs, such as in Dor Bay (Mediterranean coast; Weinstein et al., 2011), Cockburn Sound (western Australia; Loveless and Oldham, 2010), and

10   Waquoit Bay (Cape Cod, MA; Talbot et al., 2003; Gonneea and Charette, 2014). However, the groundwater-borne N load at Martinique Beach was very low in comparison to the above-mentioned sites, where fresh groundwater NO_x concentrations as high as 300 µmol L^{-1} were reported.

Estimates of nutrients export from the STE to the coastal ocean are more difficult to obtain. Direct measurements (from surface sediment incubations) are probably the most accurate ways to measure export. However, the spatial patchiness of

15   seeps at the discharge zone and the effect of tides on the hydraulic gradient in the beach aquifer lead to significant variability in direct measurements of SGD (Blanco et al., 2008; Welti et al., 2015). Furthermore, indirect estimates – based on the product of solute concentrations in fresh inland groundwater and SGD flux estimates based on isotopic tracers or hydraulic gradients – are more often used to obtain a spatially-integrated estimate of chemical discharge (Beck et al., 2011; Burnett et al., 2006), though they often ignore transformations occurring in surface sediments at the seepage face (Rao and Charette,

20   2012). Integrating the role of *in situ* N transformations is also critical to accurately estimating the impact that coastal boreal systems have on regional and global nutrient budgets. Here, the potential nutrient export from the STE at Martinique beach to the seepage face has been calculated based on Darcy's flow through the 50 m-length of the STE reported by Chaillou et al. (2016). To estimate the potential nitrogen export to the seepage face, we assumed that the TDN produced in the Martinique beach STE is flushed out of the system by the continental hydraulic gradient.

14

This potential N export corresponds to 141, 1.3 and 33.8 mol m^{-1} y^{-1} for NH$_4^+$, NO$_x$, and DON respectively (Table 3), corresponding to an annual N input of ~3100 kg along the 1200 m Martinique Beach shoreline, which is twice the fluxes from groundwater-borne. DIN exported to the seepage face (~142 mol m^{-1} y^{-1}) was in the range of previous measurements at other sites, such as the Mediterranean coast (France; 530 mol m^{-1} y^{-1}; Weinstein et al., 2011), the Gulf of Mexico (FL, USA; 414 mol m^{-1} y^{-1}; Santos et al., 2009), and the Atlantic Coast (Aquitania Coast, France; 150 mol m^{-1} y^{-1}; Anschutz et al., 2016). However, in most of these studies, DIN pool was mainly dominated by NO$_x$, while at Martinique beach NH$_4^+$ represented more than 90 % of the potential DIN supply to the seepage face. It is noteworthy that fewer studies report NH$_4^+$ as the main N species exported to the coastal ocean compared to NO$_x$. Kroeger et al. (2007) showed high proportions of NH$_4^+$ and DON in SGD fluxes to Tampa Bay (FL, USA) which may be explained in part by historical eutrophication, local hypoxia and anoxia in this area (Janicki et al., 2001). Measurements of DON flux to the coastal ocean are scarce. Kim et al. (2013) reported conservative mixing of DON, with export fluxes of 1.31×10^5 mol d^{-1} in Hwasun Bay (Jeju Island, Korea) and in the Gulf of Mexico, Santos et al. (2009) estimated that land-derived DON makes up ~52% of the total N exported to the coastal ocean.

It is difficult to estimate N fluxes by SGD to Martinique Bay, as coupled nitrification- denitrification in the upper 5-10 cm of sediments at the seepage face may remove much of the TDN flux exported from the STE (Gao et al., 2009; Gihring et al., 2010; Rao et al., 2008). Since NH$_4^+$ and DON are N species highly bioavailable to micro-organisms, this N export can further be directly transformed by the micro-phytobenthos and higher trophic levels (Miller and Ullman, 2004). While fresh inland groundwater provides few input of N to the Martinique beach, biogeochemical processes in the beach groundwater lead to the transformation of organic N to inorganic N. These biogeochemical processes affect the N species potentially discharged to the coastal ocean. This N supply from the beach groundwater could therefore change the local benthic biogeochemical cycles and associated communities (Sawyer, 2015; Welti et al., 2015).

5 Conclusion

This study highlights the role of the STE in processing groundwater-derived N in a shallow boreal STE, far from anthropogenic pressures. N was mobilized within the STE since *in situ* production of NH$_4^+$ and DON were observed in beach

groundwater. Fresh inland groundwaters delivered to the STE are rich in NO_x and DON and depleted in NH_4^+. DON represented the main N species along the flow path. However, a shift from NO_x to NH_4^+ occurred due to the removal of NO_x and the addition of NH_4^+ within the STE. Nitrate loss along the flow path could be attributed to alternative reduction pathways such as Fe oxidation and to the mineralization of OC, since DOC concentrations were high in the STE. A part of

5 NH_4^+ production could be attributed to mineralization of DON. However, the increase of TDN (i.e., DON and NH_4^+ concentration) in beach groundwater probably originated from terrestrial solid phase fraction. As a consequence, TDN in beach groundwater was higher than the inland fresh groundwater revealing the reactivity of the system. While the input of NO_x represents 32% (37 mol m^{-1} y^{-1}) of the fresh groundwater input of TDN to the STE, NO_x fluxes potentially exported from the STE to the seepage face only represent 1% of the total exported TDN. Thus, near the discharge zone, NH_4^+ and

10 DON dominated the TDN load exported to surface sediments and Martinique Bay. This local export of bioavailable N is probably removed in surface sediments, or supports benthic production and higher trophic levels. This study highlights the impact of biogeochemical transformations on N species in a boreal STE. Our study showed that biogeochemical transformations, along a continuum between fresh inland groundwater and the ocean, modify the distribution of N species, providing new N species from terrestrial origin to the coastal ocean. These biogeochemically active and dynamic systems

15 reflect the challenge of accurately estimating groundwater nutrient fluxes to the coastal ocean.

References

Abarca, E., Karam, H., Hemond, H. F. and Harvey, C. F.: Transient groundwater dynamics in a coastal aquifer: the effects of tides, the lunar cycle and the beach profile, Water Resour. Res., 49, 2473–2488, doi:10.1002/wrcr.20075, 2013.

Aller, R. C.: Bioturbation and remineralization of sedimentary organic matter: effects of redox oscillation, Chem. Geol., 114(3–4), 331–345, doi:10.1016/0009-2541(94)90062-0, 1994.

Anderson, D. M., Burkholder, J. M., Cochlan, W. P., Gobler, C. J., Heil, C. A., Kudela, R. M., Parsons, M. L., Rensel, J. E. J., Townsend, D. W., Trainer, V. L. and Vargo, G. A.: Harmful algal blooms and eutrophication: examining linkages from selected coastal regions of the United States, Harmful Algae, 8, 39–53, doi:10.1016/j.hal.2008.08.017, 2008.

Anschutz, P., Jorissen, F. J., Chaillou, G., Abu-Zied, R. and Fontanier, C.: Recent turbidite deposition in the eastern Atlantic: early diagenesis and biotic recovery, J. Mar. Res., 60(6), 835–854, doi:10.1357/002224002321505156, 2002.

Anschutz, P., Charbonnier, C., Deborde, J., Deirmendjian, L., Poirier, D., Mouret, A., Buquet, D. and Lecroart, P.: Terrestrial groundwater and nutrient discharge along the 240-km-long Aquitanian coast, Mar. Chem., na, doi:10.1016/j.marchem.2016.04.002, 2016.

Baker, M. A. and Vervier, P.: Hydrological variability, organic matter supply and denitrification in the Garonne River ecosystem, Freshw. Biol., 49(2), 181–190, doi:10.1046/j.1365-2426.2003.01175.x, 2004.

Beck, A. J., Tsukamoto, Y., Tovar-Sanchez, A., Huerta-Diaz, M., Bokuniewicz, H. J. and Sanudo-Wilhelmy, S. A.: Importance of geochemical transformations in determining submarine groundwater discharge-derived trace metal and nutrient fluxes, Appl. Geochemistry, 22, 477–490, doi:10.1016/j.apgeochem.2006.10.005, 2007.

Beck, M., Riedel, T., Graue, J., Köster, J., Kowalski, N., Wu, C. S., Wegener, G., Lipsewers, Y., Freund, H., Böttcher, M. E., Brumsack, H.-J., Cypionka, H., Rullkötter, J. and Engelen, B.: Imprint of past and present environmental conditions on microbiology and biogeochemistry of coastal Quaternary sediments, Biogeosciences, 8(1), 55–68, 2011.

Beusen, A. H. W., Slomp, C. P. and Bouwman, A. F.: Global land–ocean linkage: direct inputs of nitrogen to coastal waters via submarine groundwater discharge, Environ. Res. Lett., 8(3), 34035, doi:1748-9326/8/3/034035, 2013.

Burnett, W., Aggarwal, P., Aureli, A., Bokuniewicz, H., Cable, J., Charette, M. A., Kontar, E., Krupa, S., Kulkarni, K., Loveless, A., Moore, W., Oberdorfer, J., Oliveira, J., Ozyurt, N., Povinec, P., Privitera, A., Rajar, R., Ramessur, R., Scholten, J., Stieglitz, T., Taniguchi, M. and Turner, J.: Quantifying submarine groundwater discharge in the coastal zone via multiple methods, Sci. Total Environ., 367(2–3), 498–543, doi:10.1016/j.scitotenv.2006.05.009, 2006.

Chaillou, G., Anschutz, P., Dubrulle, C. and Lecroart, P.: Transient states in diagenesis following the deposition of a gravity layer: dynamics of O2, Mn, Fe and N-species in experimental units, Aquat. Geochemistry, 13(2), 157–172, doi:10.1007/s10498-007-9013-0, 2007.

Chaillou, G., Touchette, M., Rémillard, A., Buffin-Bélanger, T., St-Louis, R., Hétu, B. and Tita, G.: Synthèse de l'état des connaissances sur les eaux souterraines aux Îles-de-la-Madeleine - Impacts de l'exploration et de l'exploitation des ressources naturelles sur celles-ci., 2012.

Chaillou, G., Couturier, M., Tommi-Morin, G. and Rao, A. M. .: Total alkalinity and dissolved inorganic carbon production in groundwaters discharging through a sandy beach, Procedia Earth Planet. Sci., 10, 88–99, doi:10.1016/j.proeps.2014.08.017, 2014.

Chaillou, G., Lemay-Borduas, F. and Couturier, M.: Transport and transformations of groundwater-borne carbon discharging through a sandy beach to coastal ocean, Can. Water Resour. J., 38(2), 809–828, doi:10.1080/07011784.2015.1111775, 2016.

Chaillou, G., Lemay-Borduas, F., Larocque, M., Couturier, M., Biehler, A. and Tommi-Morin, G.: Flow and discharge of groundwater from a snowmelt-affected sandy beach, J. Hydrol., n.d.

Couturier, M., Nozais, C. and Chaillou, G.: Microtidal subterranean estuaries as a source of fresh terrestrial dissolved organic matter to coastal ocean, Mar. Chem., 186, 46–57, doi:10.1016/j.marchem.2016.08.001, 2016.

Cyronak, T., Santos, I. R., Erler, D. V. and Eyre, B. D.: Groundwater and porewater as major sources of alkalinity to a fringing coral reef lagoon (Muri Lagoon, Cook Islands), Biogeosciences, 10(4), 2467–2480, doi:10.5194/bg-10-2467-2013, 2013.

Erler, D. V, Santos, I. R., Zhang, Y., Tait, D. R., Befus, K. M., Hidden, A., Li, L. and Eyre, B. D.: Nitrogen transformations within a tropical subterranean estuary, Mar. Chem., 164, 38–47, doi:10.1016/j.marchem.2014.05.008, 2014.

Gao, H., Schreiber, F., Collins, G., Jensen, M. M., Kostka, J. E., Lavik, G., de Beer, D., Zhou, H. and Kuypers, M. M.: Aerobic denitrification in permeable Wadden Sea sediments, ISME J., 4(3), 417–426, doi:10.1038/ismej.2009.127, 2009.

Gehrels, W. R.: Determining relative sea-level change from salt-marsh foraminifera and plant zones on the coast of Maine, USA, J. Coast. Res., 10(4), 990–1009, doi:0749-0208, 1994.

Gihring, T. M., Canion, A., Riggs, A., Huettel, M. and Kostka, J. E.: Denitrification in shallow, sublittoral Gulf of Mexico permeable sediments, Limnol. Oceanogr., 55(1), 43–54, doi:10.4319/lo.2010.55.1.0043, 2010.

Glibert, P. M., Icarus Allen, J., Artioli, Y., Beusen, A., Bouwman, L., Harle, J., Holmes, R. and Holt, J.: Vulnerability of coastal ecosystems to changes in harmful algal bloom distribution in response to climate change: projections based on model analysis, Glob. Chang. Biol., 20(12), 3845–3858, doi:10.1111/gcb.12662, 2014.

Gonneea, M. E. and Charette, M. A.: Hydrologic controls on nutrient cycling in an unconfined coastal aquifer, Environ. Sci. Technol., 48, 14178–14185, doi:10.1021/es503313t, 2014.

Gonneea, M. E., Mulligan, A. E. and Charette, M. A.: Climate-driven sea level anomalies modulate coastal groundwater dynamics and discharge, Geophys. Res. Lett., 40(11), 2701–2706, doi:10.1002/grl.50192, 2013.

Hall, P. J. and Aller, R. C.: Rapid, small-Volume, flow injection analysis for CO_2 and NH_4+ in marine and freshwaters, Limnol. Oceanogr., 37(5), 1113–1119, 1992.

Hansell, D. A. and Carlson, C. A.: Biogeochemistry of marine dissolved organic matter., 2014.

Heiss, J. W. and Michael, H. A.: Saltwater-freshwater mixing dynamics in a sandy beach aquifer over tidal, srping-neap and seasonal cycles, Water Resour. Res., 50, 6747–6766, doi:10.1002/2014WR015574, 2014.

Hinzman, L. D., Bettez, N. D., Bolton, W. R., Chapin, F. S., Dyurgerov, M. B., Fastie, C. L., Griffith, B., Hollister, R. D., Hope, A., Huntington, H. P., Jensen, A. M., Jia, G. J., Jorgenson, T., Kane, D. L., Klein, D. R., Kofinas, G., Lynch, A. H.,

Lloyd, A. H., Mcguire, A. D., Nelson, F. E., Oechel, W. C., Osterkamp, T. E., Racine, C. H., Romanovsky, V. E., Stone, R. S., Stow, D. A., Sturm, M., Tweedie, C. E., Vourlitis, G. L., Walker, M. D., Walker, D. A., Webber, P. J., Welker, J. M., Winker, K. S. and Yoshikawa, K.: Evidence and implications of recent climate change in northern Alaska and other Arctic regions, Clim. Change, 72(3), 251–298, doi:10.1007/s10584-005-5352-2, 2005.

5 Howarth, R. W. and Marino, R.: Nitrogen as the limiting nutrient for eutrophication in coastal marine ecosystems: evolving views over three decades, Limnol. Oceanogr., 51(1) part.2), 364–376, doi:10.4319/lo.2006.51.1_part_2.0364, 2006.

Hulth, S., Aller, R. C. and Gilbert, F.: Coupled anoxic nitrification/manganese reduction in marine sediments, Geochim. Cosmochim. Acta, 63(1), 49–66, doi:10.1016/S0016-7037(98)00285-3, 1999.

Hyacinthe, C., Anschutz, P., Carbonel, P., Jouanneau, J. M. and Jorissen, F. J.: Early diagenetic processes in the muddy
10 sediments of the bay of biscay, Mar. Geol., 177(1–2), 111–128, doi:10.1016/S0025-3227(01)00127-X, 2001.

Jackson, N. ., Nordstrom, K. ., Smith, D. . and Virginia, W.: Geomorphic – biotic interactions on beach foreshores in estuaries, J. Coast. Res., 424(36), 414–424, doi:0749-0208, 2002.

Janicki, A., Pribble, R., Janicki, S. and Winowitch, M.: An analysis of long-term trends in Tampa Bay water quality., 2001.

Johannes, R. E.: The ecological significance of the submarine discharge of groundwater, Mar. Ecol. Prog. Ser., 3, 365–373,
15 doi:0171-8630/80/0003/0365, 1980.

Jørgensen, L., Lechtenfeld, O., Benner, R., Middelboe, M. and Stedmon, C. A.: Bacterial production and transformation of dissolved neutral sugars and amino acids in seawater, Biogeosciences Discuss., 11(4), 6151–6184, doi:10.5194/bgd-11-6151-2014, 2014.

Juneau, M.-N.: Hausse récente du niveau marin relatif aux Îles de la Madeleine, Master's thesis, Université du Québec à
20 Rimouski, Rimouski., 2012.

Kelaher, B. and Levinton, J.: Variation in detrital enrichment causes spatio-temporal variation in soft-sediment assemblages, Mar. Ecol. Prog. Ser., 261, 85–97, doi:10.3354/meps261085, 2003.

Kim, T., Kwon, E., Kim, I., Lee, S. and Kim, G.: Dissolved organic matter in the subterranean estuary of a volcanic island, Jeju: importance of dissolved organic nitrogen fluxes to the ocean, J. Sea Res., 78, 18–24, doi:10.1016/j.seares.2012.12.009,
25 2013.

Knee, K. L. and Jordan, T. E.: Spatial distribution of dissolved radon in the Choptank river and its tributaries: implications for groundwater discharge and nitrate inputs, Estuaries and Coasts, 36, 1237–1252, 2013.

Korom, S. F.: Natural denitrification in the saturated zone: a review, Water Resour. Res., 28(6), 1657–1668, doi:10.1029/92WR00252, 1992.

30 Kroeger, K. D. and Charette, M.: Nitrogen biogeochemistry of submarine groundwater discharge, Limnol. Oceanogr., 53(3), 1025–1039, 2008.

Kroeger, K. D., Cole, M. L. and Valiela, I.: Groundwater-transported dissolved organic nitrogen exports from coastal watersheds, Limnol. Oceanogr., 51(5), 2248–2261, doi:10.4319/lo.2006.51.5.2248, 2006.

Kroeger, K. D., Swarzenski, P. W., Greenwood, W. J. and Reich, C.: Submarine groundwater discharge to Tampa Bay:

nutrient fluxes and biogeochemistry of the coastal aquifer, Mar. Chem., 104(1–2), 85–97, doi:10.1016/j.marchem.2006.10.012, 2007.

Loveless, A. M. and Oldham, C. E.: Natural attenuation of nitrogen in groundwater discharging through a sandy beach, Biogeochemistry, 98(1–3), 75–87, doi:10.1007/s10533-009-9377-x, 2010.

5   Madelin'Eau: Gestion des eaux souterraines aux Îles-de-la-Madeleine Un défi de développement durable Rapport final., 2004.

Madelin'Eau: Secteur sud-est de l'île de grande entrée- Rapport hydrologique., 2007.

Madelin'Eau: Secteur de grande-entrée- flanc nord alimentation en eau potable., 2009.

Madelin'Eau: Projet de réalisation d'un forage gazier vertical et conventionel d'une profondeur de 2500 m, municipalité des

10   îles de la Madeleine- Rapport d'étape 1, expertise hydrogéologique., 2011.

Martin, J. B., Hartl, K. M., Corbett, D. R., Swarzenski, P. W. and Cable, J. E.: A multi-level pore-water sampler for permeable sediments, J. Sediment. Res., 73(1), 128–132, doi:10.1306/070802730128, 2003.

Masselink, G. and Short, A.: The effect on tide range on beach morphodynamics and morphology: a conceptual beach model, J. Coast. Res., 9(3), 785–800, 1993.

15   McCoy, C. and Corbett, D. R.: Review of submarine groundwater discharge (SGD) in coastal zones of the Southeast and Gulf Coast regions of the United States with management implications, J. Environ. Manage., 90(1), 644–51, doi:10.1016/j.jenvman.2008.03.002, 2009.

Miller, D. C. and Ullman, W. J.: Ecological consequences of ground water discharge to Delaware Bay, United States, Groundwater, 42(7), 959–970, doi:10.1111/j.1745-6584.2004.tb02635.x, 2004.

20   Moore, W. S.: The subterranean estuary: a reaction zone of ground water and sea water, Mar. Chem., 65(1–2), 111–125, doi:10.1016/S0304-4203(99)00014-6, 1999.

Moore, W. S.: The effect of submarine groundwater discharge on the ocean., Ann. Rev. Mar. Sci., 2, 59–88, doi:10.1146/annurev-marine-120308-081019, 2010.

Null, K. A., Dimova, N. T., Knee, K. L., Esser, B. K., Swarzenski, P. W., Singleton, M. J., Stacey, M. and Paytan, A.:

25   Submarine groundwater discharge-derived nutrient loads to San Francisco bay: implications to future ecosystem changes, Estuaries and Coasts, 35(5), 1299–1315, doi:10.1007/s12237-012-9526-7, 2012.

Postma, D.: Kinetics of nitrate reduction by detrital Fe (II)-silicates, Geochim. Cosmochim. Acta, 54(3), 903–908, 1990.

Postma, D., Boesen, C., Kristiansen, H. and Larsen, F.: Nitrate reduction in an unconfined sandy aquifer: water chemistry, reduction processes and geochemical modeling, Water Resour. Res., 27(8), 2027–2045, doi:0043-1397/91/91, 1991.

30   Rao, A. M. F. and Charette, M. A.: Benthic nitrogen fixation in an eutrophic estuary affected by groundwater discharge, J. Coast. Res., 280(2), 477–485, doi:10.2112/JCOASTRES-D-11-00057.1, 2012.

Rao, A. M. F., McCarthy, M. J., Gardner, W. S. and Jahnke, R. a.: Respiration and denitrification in permeable continental shelf deposits on the South Atlantic Bight: N2: Ar and isotope pairing measurements in sediment column experiments, Cont. Shelf Res., 28(4–5), 602–613, 2008.

Rivett, M. O., Buss, S. R., Morgan, P., Smith, J. W. N. and Bemment, C. D.: Nitrate attenuation in groundwater: A review of biogeochemical controlling processes, Water Res., 42(16), 4215–4232, doi:10.1016/j.watres.2008.07.020, 2008.

Robinson, C., Li, L. and Barry, D. A.: Effect of tidal forcing on a subterranean estuary, Adv. Water Resour., 30(4), 851–865, doi:10.1016/j.advwatres.2006.07.006, 2007a.

Robinson, C., Li, L. and Prommer, H.: Tide-induced recirculation across the aquifer-ocean interface, Water Resour. Res., 43(7), 6–14, doi:10.1029/2006WR005679, 2007b.

Robinson, C., Xin, P., Li, L. and Barry, D. A.: Groundwater flow and salt transport in a subterranean estuary driven by intensified wave conditions, Water Resour. Res., 50(1), 165–181, doi:10.1002/2013WR013813, 2014.

Rocha, C., Ibanhez, J. and Leote, C.: Benthic nitrate biogeochemistry affected by tidal modulation of Submarine Groundwater Discharge (SGD) through a sandy beach face, Ria Formosa, Southwestern Iberia, Mar. Chem., 115(1–2), 43–58, doi:10.1016/j.marchem.2009.06.003, 2009.

Rocha, C., Wilson, J., Scholten, J. and Schubert, M.: Retention and fate of groundwater-borne nitrogen in a coastal bay (Kinvara Bay, Western Ireland) during summer, Biogeochemistry, 125(2), 275–299, doi:10.1007/s10533-015-0116-1, 2015.

Rossi, F., Incera, M., Callier, M. and Olabarria, C.: Effects of detrital non-native and native macroalgae on the nitrogen and carbon cycling in intertidal sediments, Mar. Biol., 158(12), 2705–2715, doi:10.1007/s00227-011-1768-6, 2011.

Sáenz, J. P., Hopmans, E. C., Rogers, D., Henderson, P. B., Charette, M. A., Schouten, S., Casciotti, K. L., Sinninghe Damsté, J. S. and Eglinton, T. I.: Distribution of anaerobic ammonia-oxidizing bacteria in a subterranean estuary, Mar. Chem., 136, 7–13, doi:10.1016/j.marchem.2012.04.004, 2012.

Santoro, A. E.: Microbial nitrogen cycling at the saltwater-freshwater interface, Hydrogeol. J., 18, 187–202, doi:10.1007/s10040-009-0526-z, 2010.

Santos, I., Burnett, W. C., Dittmar, T., Suryaputra, I. G. N. and Chanton, J.: Tidal pumping drives nutrient and dissolved organic matter dynamics in a Gulf of Mexico subterranean estuary, Geochim. Cosmochim. Acta, 73(5), 1325–1339, doi:10.1016/j.gca.2008.11.029, 2009.

Santos, I., Eyre, B. D. and Huettel, M.: The driving forces of porewater and groundwater flow in permeable coastal sediments: A review, Estuar. Coast. Shelf Sci., 98, 1–15, doi:10.1016/j.ecss.2011.10.024, 2012.

Santos, I. R.: Submarine groundwater discharge driving mechanisms and biogeochemical aspects, The Florida State University., 2008.

Santos, I. R., Burnett, W. C., Chanton, J., Mwashote, B., Suryaputra, I. G. N. A. and Dittmar, T.: Nutrient biogeochemistry in a Gulf of Mexico subterranean estuary and groundwater-derived fluxes to the coastal ocean, Limnol. Oceanogr., 53(2), 705–718, doi:10.4319/lo.2008.53.2.0705, 2008.

Santos, I. R., Bryan, K. R., Pilditch, C. A. and Tait, D. R.: Influence of porewater exchange on nutrient dynamics in two New Zealand estuarine intertidal flats, Mar. Chem., 167, 57–70, doi:10.1016/j.marchem.2014.04.006, 2014.

Sawyer, A. H.: Enhanced removal of groundwater-borne nitrate in heterogeneous aquatic sediments, Geophys. Res. Lett., 42(2), 403–410, doi:10.1002/2014GL062234, 2015.

Schlacher, T. A. and Connolly, R. M.: Land–ocean coupling of carbon and nitrogen fluxes on sandy beaches, Ecosystems, 12(2), 311–321, doi:10.1007/s10021-008-9224-2, 2009.

Schnetger, B. and Lehners, C.: Determination of nitrate plus nitrite in small volume marine water samples using vanadium(III)chloride as a reduction agent, Mar. Chem., 160, 91–98, doi:10.1016/j.marchem.2014.01.010, 2014.

5 Scott, D. B., Brown, K., Collins, E. S. and Medioli, F. S.: A new sea-level curve from Nova Scotia: evidence for a rapid acceleration of sea-level rise in the late mid-Holocene, Can. J. Earth Sci., 32(12), 2071–2080, doi:10.1139/e95-160, 1995a.

Scott, D. B., Gayes, P. T. and Collins, E. S.: Mid-holocene precedent for a future rise in sea-level along the Atlantic coast of North America, J. Coast. Res., 11(3), 615–622, doi:4298366, 1995b.

Seitzinger, S. P., Sanders, R. W. and Styles, R.: Bioavailability of DON from natural and anthropogenic sources to estuarine
10 plankton, Limnol. Oceanogr., 47(2), 353–366, doi:10.4319/lo.2002.47.2.0353, 2002.

Seitzinger, S. P., Harrison, J. A., Dumont, E., Beusen, A. H. W. and Bouwman, A. F.: Sources and delivery of carbon, nitrogen and phosphorus to the coastal zone: an overview of global Nutrient Export from Watersheds (NEWS) models and their application, Global Biogeochem. Cycles, 19(4), GB4S01, doi:10.1029/2005GB002606, 2005.

Sipler, R. E. and Bronk, D. A.: Dynamics of dissolved organic nitrogen, in Biogeochemistry of marine dissolved organic
15 matter, edited by D. A. Hansell and C. A. Carlson, pp. 127–184, Academic Press., 2014.

Slomp, C. P. and Van Cappellen, P.: Nutrient inputs to the coastal ocean through submarine groundwater discharge: controls and potential impact, J. Hydrol., 295(1–4), 64–86, doi:10.1016/j.hydrol.2004.02.018, 2004.

Sundby, B.: Transient state diagenesis in continental margin muds, Mar. Chem., 102(1–2), 2–12, doi:10.1016/j.marchem.2005.09.016, 2006.

20 Talbot, J. M., Kroeger, K. D., Rago, A., Allen, M. C. and Charette, M. A.: Nitrogen flux and speciation through the subterranean estuary of Waquoit Bay, Massachusetts, Biol. Bull., 205(2), 244–245, doi:10.2307/1543276, 2003.

Valiela, I., Costa, J., Foreman, K., Teal, J. M., Howes, B. and Aubrey, D.: Transport of groundwater-borne nutrients from watersheds and their effects on coastal waters, Biogeochemistry, 10, 177–197, 1990.

Voss, M., Bange, H. W., Dippner, J. W., Middelburg, J. J., Montoya, J. P. and Ward, B.: The marine nitrogen cycle: recent
25 discoveries, uncertainties and the potential relevance of climate change, Philos. Trans. R. Soc., 368, 20130121, 2013.

Weinstein, Y., Yechieli, Y., Shalem, Y., Burnett, W., Swarzenski, P. W. and Herut, B.: What is the role of fresh groundwater and recirculated seawater in conveying nutrients to the coastal ocean ?, Environ. Sci. Technol., 45, 5195–5200, doi:10.1021/es104394r, 2011.

Welti, N., Gale, D., Hayes, M., Kumar, A., Gasparon, M., Gibbes, B. and Lockington, D.: Intertidal diatom communities
30 reflect patchiness in groundwater discharge, Estuar. Coast. Shelf Sci., doi:10.1016/j.ecss.2015.06.006, 2015.

Table 1: Mean concentrations (μmol L^{-1}) of nitrogen species in the groundwater and seawater end-members as well as ranges in beach groundwater measured during the study. NO_x and NH_4^+ was measured in 2011, 2012, 2013 and 2015, and TDN and DON was measured in 2012.

	Inland wells	Seawater	Beach groundwater
2011–2015	N=10	N=6	N=245
NO_x	65.5 ± 26.7	0.5 ± 0.5	0–26.1
NH_4^+	0.1 ± 0.3	0.8 ± 0.5	0.1–1056.2
2012	N=2	N=3	N=54
DON	110.9 ± 3.4	7.3 ± 0.8	0–1481.8
TDN	203 ± 4.5	9.1 ± 1.1	7.4–1704.4

Table 2: Nutrient inventories estimated along the STE. Inventories were calculated in fresh, brackish and saline beach groundwater, the 2013 data set was used. For dissolved organic nitrogen, concentrations measured in 2012 were used.

	N	Inventories [μmol m^{-2}]				
Beach groundwater		NH_4^+	NO_3^-	DIN	DON[a]	TDN[a]
Fresh water (S<5)	57	16	0.1	16.1	18.7	34.8
Brackish water (5<S<15)	19	27.3	0.3	27.6	23.9	51.5
Saline water (S>15)	15	14.8	0.1	15	8.9	24

[a] Calculated on 2012 sampling

Table 3: N fluxes delivery to STE and exported to coastal ocean in mol m^{-1} y^1. Fresh inland groundwater –borne fluxes was computed as the product of average concentrations of N in groundwater end-member and the volume of fresh groundwater discharge (Q_{inland}). The exported N fluxes were the product of N inventory at the high tide mark and the flow measured in the beach (Q_{beach}). Inorganic N fluxes were estimated on 2013 sampling and DON fluxes were based on 2012 sampling.

Fluxes mol m^{-1} y^{-1}	NH_4^+	NO_x	DIN	DON[a]
Fresh inland groundwater	0.07	37	37	63
Exported N	141	1.3	142.3	33.8

[a] Calculated on 2012 sampling with hydrologic flow determined in 2013

Figures captions

Figure 1: Position of the study site in the Magdalen Islands (Québec, Canada) (A, B). (C) Beach profile of the Martinique beach in 2011, 2012, 2013 and 2015; beach profiles were determined using a DGPS; Locations of sampling sites (2011–2013, 2015) along the sandy beach transect. Depths are relative to mean sea level (i.e., 0 m is mean sea level) (C).

5

Figure 2: Cross-sections of the transect (see Fig. 1C) showing the beach profile and mean distribution of salinity and dissolved oxygen in 2011, 2012, 2013, and 2015 (no dissolved oxygen data are available for 2015). Depths are relative to mean sea level (i.e., 0 m is mean sea level). Contour lines were derived by spatial interpolation (kriging method) of data points; the interpolation model reproduced the empirical data set with a 97% confidence level. White dots represent the
10   depths at which samples were collected using multi-level samplers. The dashed line represents the water table level.

Figure 3: Cross-sections of the transect (see Fig. 1C) showing the beach profile and distributions of (A) nitrate + nitrite (NO_x) and (B) ammonium in μmol L^{-1} in 2011, 2012, 2013 and 2015. Black contour lines refer to salinity. Depths are relative to mean sea level (i.e., 0 m is mean sea level). All contour lines were derived by spatial interpolation (kriging
15   method) of data points. White dots represent the depths at which samples were collected using multi-level samplers.

Figure 4: Cross-sections of the transect (see Fig. 1C) showing the topography and distributions of DON and TDN in μmol L^{-1} in 2012. Black contour lines refer to salinity. Depths are relative to mean sea level (i.e., 0 m is mean sea level). All contour lines were derived by spatial interpolation (kriging method) of data points. White dots represent the depths at which samples
20   were collected using multi-level samplers.

Figure 5: Distribution of NO_x and NH_4^+ groundwater concentration in μmol L^{-1} collected in 2011, 2012, 2013, and 2015 (A, B) and DON and TDN in 2012 (C, D) within the STE relative to salinity grouped for different DO saturation from 0-20%, 20-60% and 60-100%. Extra points are not included to allow a better visibility. Black dots were used when no data on DO
25   saturation were available. Red triangles are mean groundwater end-member values and black squares are mean seawater end-member values. Standard deviations are black lines associated with end-members. Dashed lines represent the theoretical mixing line between groundwater and seawater end-members.

Figure 6: Cross-sections of the transect (see Fig. 1C) showing the topography and distributions of dissolved iron in μmol L^{-1}
30   in 2011, 2012, 2013 and 2015. White contour lines refer to salinity. Depths are relative to mean sea level (i.e., 0 m is mean sea level). All contour lines were derived by spatial interpolation (kriging method) of data points. White dots represent the depths at which samples were collected using multi-level samplers.

Figure 7: Schematic representation of 1) N inventories in fresh, brackish and saline beach groundwater (boxes from light grey to dark grey respectively), dashed lines represent the schematic salinity separation. 2) fresh inland groundwater fluxes and potential exported fluxes to coastal water (white boxes). White arrow schematizes the groundwater flow path from the inland groundwater to the seepage face.
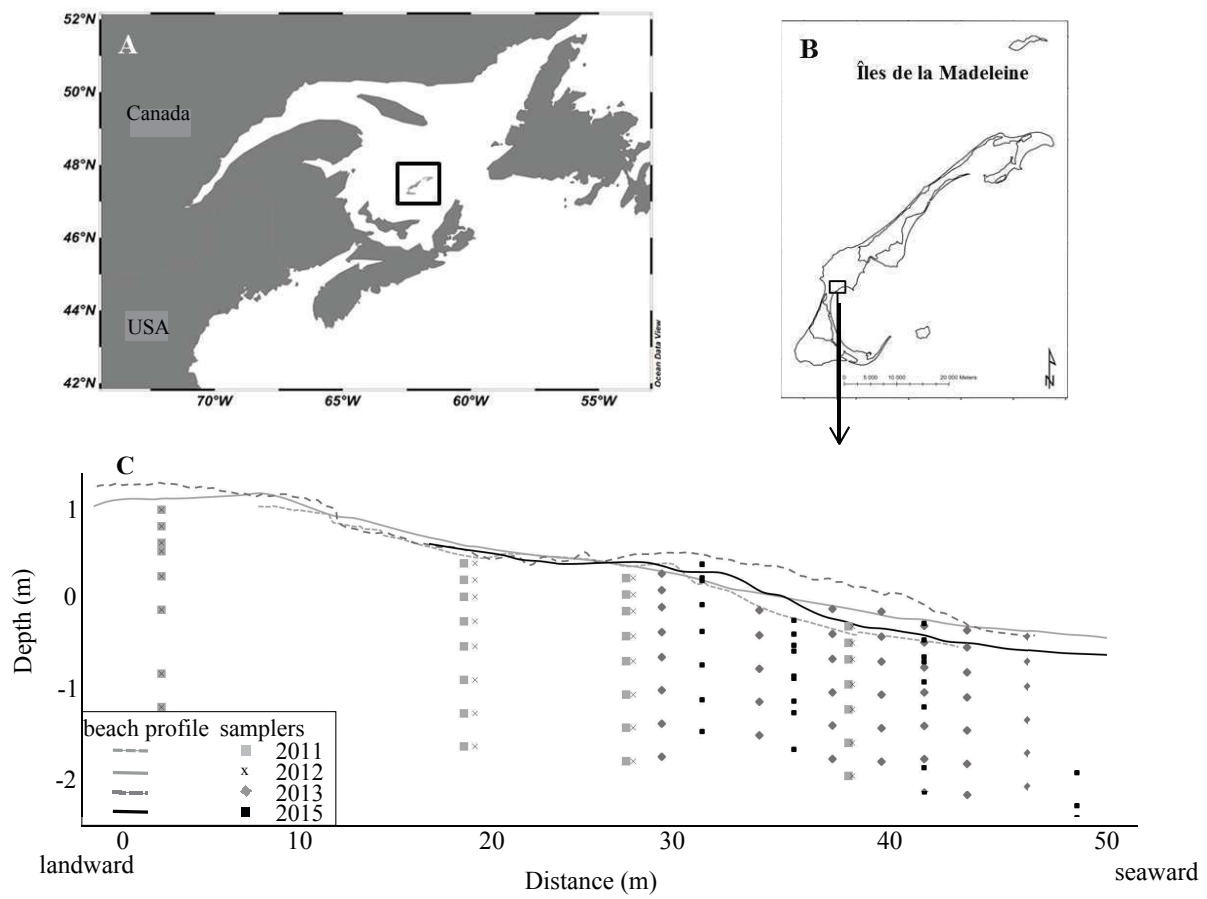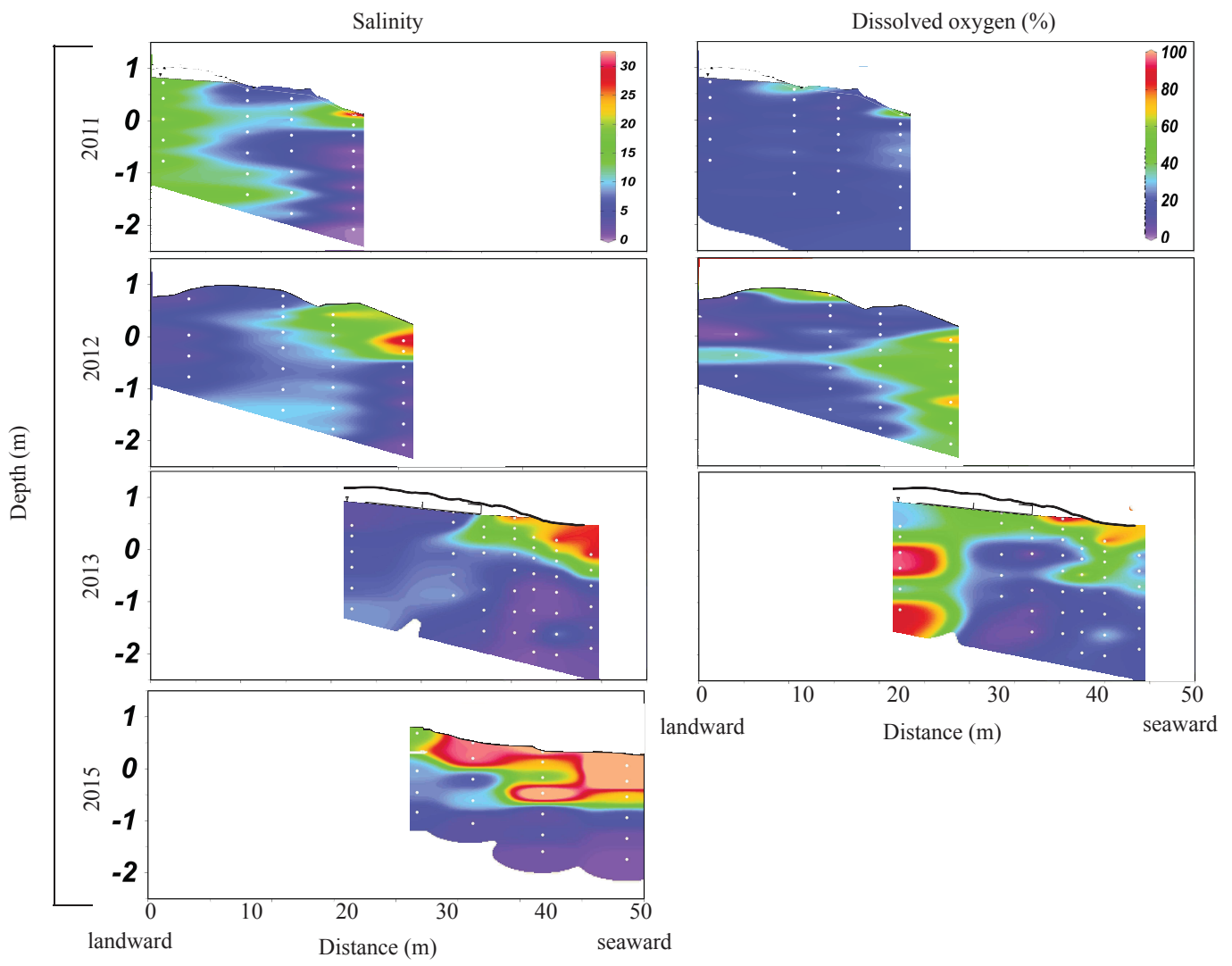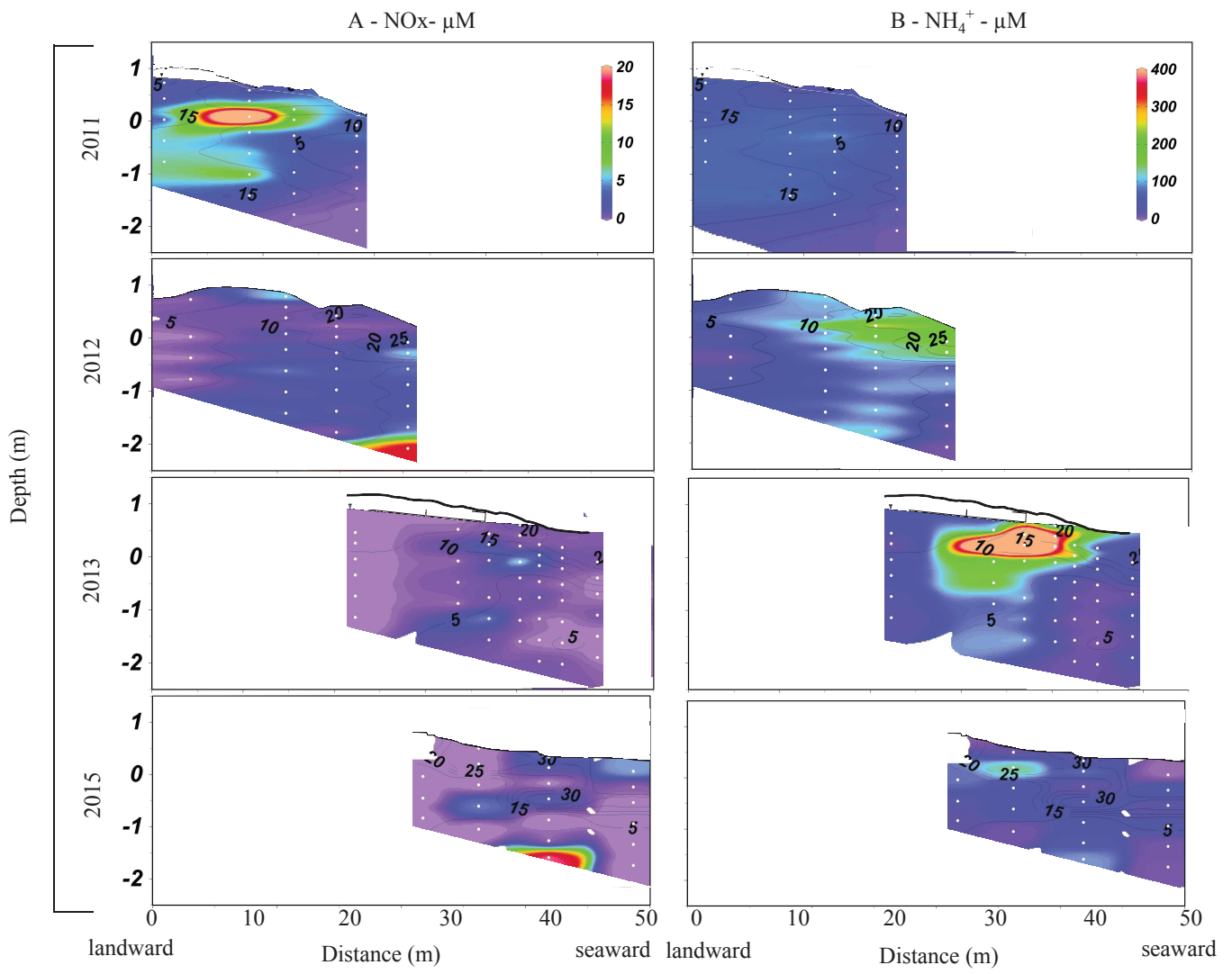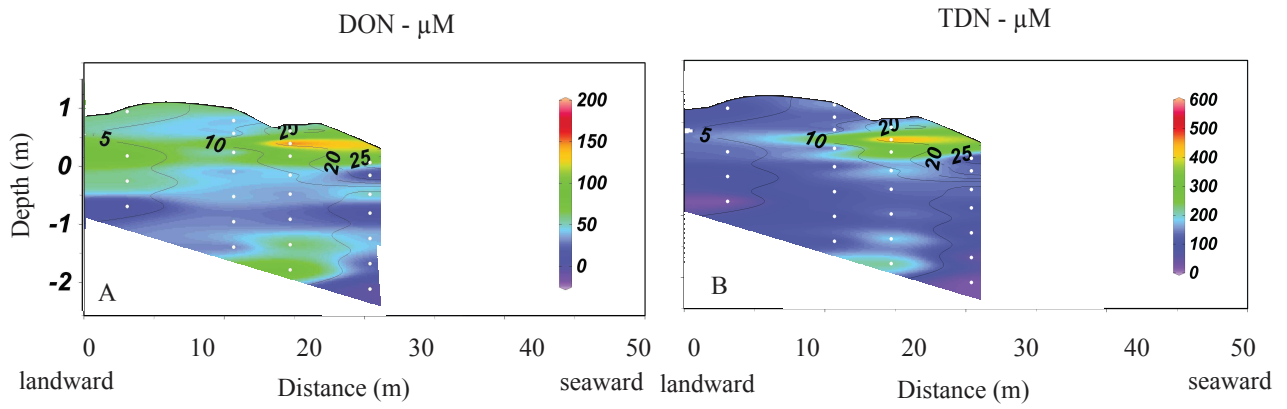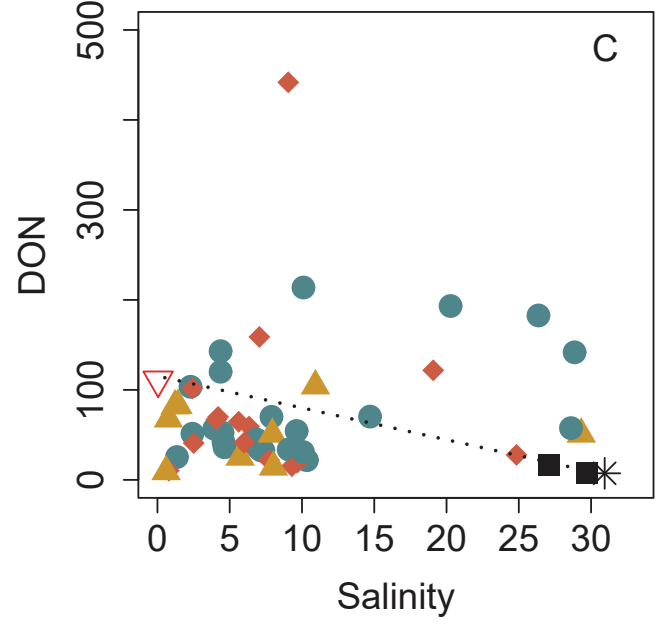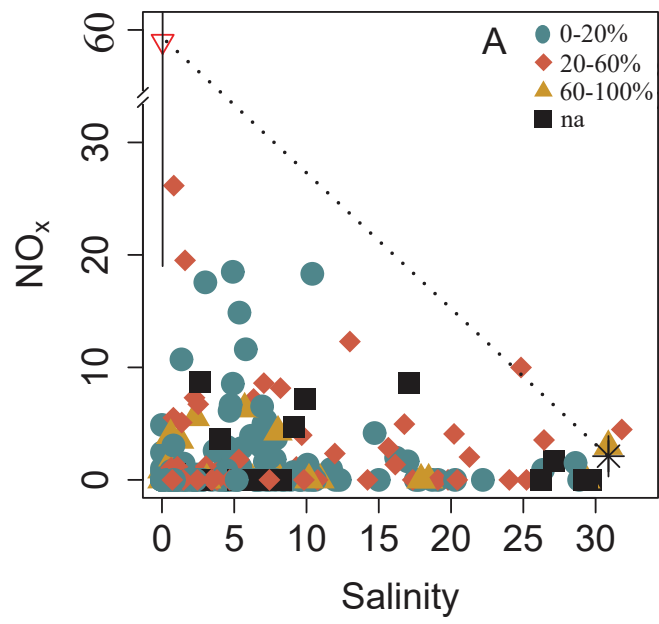
5

Figure 1

Figure 2

Figure 3

2012

DON - µM

TDN - µM

Figure 4

Figure 5

Figure 6

Potential Fluxes to coastal water mol m^{-1} y^{-1}

NH$_4^+$	141
NO$_x$	1.3
DON	33.8

Saline groundwater inventories

NH$_4^+$	14.82
NO$_x$	0.13
DON	8.9

Brackish groundwater inventories

NH$_4^+$	27.3
NO$_x$	0.3
DON	23.9

Fresh groundwater inventories

NH$_4^+$	16
NO$_x$	0.1
DON	18.7

Fresh inland groundwater mol m^{-1} y^{-1}

NH$_4^+$	0.07
NO$_x$	37.54
DON	63.57

Figure 7